

Bloch Oscillations in the Presence of Plasmons and Phonons

Avik W. Ghosh,* Lars Jönsson, and John W. Wilkins

Department of Physics, The Ohio State University, 174 West 18th Avenue, Columbus, Ohio 43210
(Received 22 October 1999)

The coupling between Bloch oscillating electrons and longitudinal optical phonons in a superlattice leads to resonant phonon excitation but no gap in the Bloch-phonon spectrum. In addition, we predict a sharp transition from plasma to Bloch oscillations at $\nu_B = 2\nu_p$. From a microscopic description with phenomenological dampings, we numerically map out the behavior of coupled Bloch-plasmon-phonon modes for a wide range of parameters, and mimic experimental conditions. Our results are in good agreement with recent experiments by Dekorsy *et al.* [Phys. Rev. Lett. **85**, 1080 (2000)].

PACS numbers: 72.20.Jv, 73.23.Ad, 78.47.+p

In a constant electric field and in the absence of collisions, a quantum particle in a periodic potential executes Bloch oscillations [1]. Bloch oscillations have been observed experimentally in a variety of systems [2–4], including superlattices at room temperature [5]. The proportionality of the Bloch frequency to the electric field makes the oscillations tunable, and thus a potential source of coherent THz radiation [6]. Tuning the Bloch oscillator, however, brings it in resonance with other oscillation modes in superlattices, such as plasmons and longitudinal optical (LO) phonons. The coupling of a Bloch oscillator with such modes contributes strongly to the dephasing of the Bloch oscillations, and is therefore a crucial factor in limiting the efficiency of room-temperature THz devices.

When two oscillation modes are resonant, the behaviors of the coupled modes are markedly different from each individual mode. In plasmon-phonon modes, for example [7], the linear coupling between plasmons and LO phonons leads to a gap between the individual modes at resonance. One might expect an analogous gap at resonance between Bloch oscillations and phonons. In this Letter, we show that the coupling of Bloch oscillation and phonon modes (i) does *not* lead to a gap but (ii) produces a strong resonant enhancement of the phonon amplitude. These results are in agreement with recent experiments by Dekorsy *et al.* [8]. In addition, in the absence of collisions as the electric field is varied, we predict a sharp transition from the low field (coupled plasmon-phonon) to the high field (Bloch-phonon) mode. The complete spectrum of Bloch-plasmon-phonon modes is shown in Fig. 1.

Microscopic theory.—With units $\hbar = e = 1$ in this section, we consider superlattice (period d) electrons of density n with tight-binding energy $\epsilon_k = -(\Delta/2)\cos kd$ and Coulomb repulsion $V_q = 4\pi/q^2$ in an external dc electric field E_0 along the growth direction. Dispersionless LO phonons, ω_{LO} , couple to the electrons via a Fröhlich interaction $M_q = -i\sqrt{2\pi}\omega_{LO}[1/\epsilon_\infty - 1/\epsilon_0]/q$, where ∞ and 0 designate the high and low frequency dielectric constants. The Hamiltonian is [9]

$$\begin{aligned}
 H = & \sum_k \epsilon_k c_k^\dagger c_k + \frac{1}{2} \sum_{qkk'} V_q c_{k+q}^\dagger c_{k'-q}^\dagger c_k' c_k \\
 & - E_0 \sum_{kk'} \mu_{kk'} c_k^\dagger c_{k'} + \sum_q \omega_{LO} b_q^\dagger b_q \\
 & - E_0 \sum_q \mu_q (b_q + b_q^\dagger) \\
 & + \sum_{kq} M_q c_k^\dagger c_{k+q} (b_q + b_{-q}^\dagger), \quad (1)
 \end{aligned}$$

with $\mu_{kk'} = i\delta_{kk'}\partial/\partial k$ the electron dipole matrix [10] and μ_q the phonon dipole moment.

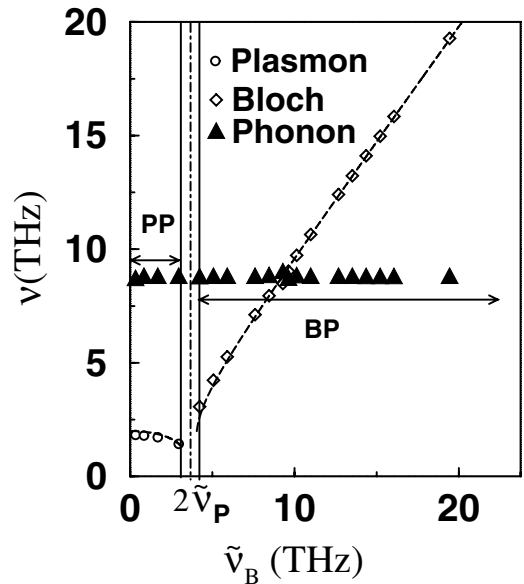


FIG. 1. Coexistence of all three modes at $\nu_p = \omega_p/2\pi = 2$ THz: coupled plasmon-phonon modes (PP) for $\tilde{\nu}_B = \tilde{\omega}_B/2\pi < 2\tilde{\nu}_p$ [15], and Bloch-phonon modes (BP) above. The dashed lines are predictions from the pendulum equation (4) while the symbols arise from the numerical solution of Eq. (5). The sharp transition between the modes occurs in the absence of collisions. The motion of the electron is aperiodic near the transition point, so only frequencies outside the solid vertical lines can be resolved.

Discarding correlations [11,12], we factorize all four-operator expectation values by products of two-operator values. The dynamics is then described by the polarization $P = i \sum_K \partial N_{KQ} / \partial Q|_{Q=0}$ where $N_{KQ} \equiv \langle c_{K+Q/2}^\dagger c_{K-Q/2} \rangle$ is the electron density matrix and $K = (k + k')/2$ and $Q = k - k'$ are the “center-of-mass” and “relative” momenta. The polarization evolves as $\partial P / \partial t = \sum_K N_{K0} \partial \epsilon_K / \partial K$ [10], and the evolution of N_{K0} obtained from H is

$$\begin{aligned} & \left[\frac{\partial}{\partial t} + (E_0 - 4\pi P) \frac{\partial}{\partial K} \right] N_{K0} \\ &= -i \sum_q M_q (B_q + B_{-q}^*) [N_{K-q/2,q} - N_{K+q/2,q}], \end{aligned} \quad (2)$$

where $B_q = \langle b_q \rangle$ is the amplitude of the *coherent* phonons. For $q \rightarrow 0$, we obtain $[\partial / \partial t + E(t) \partial / \partial K] N_{K0} = 0$, where the total field $E(t) = E_0 - 4\pi P - Cw/d$, $C = \sqrt{\omega_{LO}^2 - \omega_{TO}^2}$, $w = d\sqrt{8\pi/\epsilon_\infty} \text{Re} B_0$, and $\omega_{LO}/\omega_{TO} = \sqrt{\epsilon_0/\epsilon_\infty}$ (Lyddane-Sachs-Teller relation [13]). The solution is $N_{K0}(t) = f(K - \eta(t)/d)$, where f is the initial distribution function and $\eta = d \int_0^t E(t) dt$.

This solution for N_{K0} and the equation for $P(t)$, assuming a flat initial distribution f between $\pm K_F$ ($\ll 1/d$), yields a nonlinear pendulum equation for η . A similar analysis for w leads to a coupling of the nonlinear pendulum (electron) with a linear oscillator (phonon):

$$\ddot{\eta} + \omega_p^2 \sin \eta = -C \dot{w}; \quad \ddot{w} + \omega_{TO}^2 w = C \dot{\eta}, \quad (3)$$

where the plasma frequency $\omega_p \equiv \sqrt{4\pi n e^2 / m^*}$, and m^* is the electron effective mass.

Bloch plasmons.—Without phonons we obtain a pendulum equation [14]:

$$\ddot{\eta} + \omega_p^2 \sin \eta = 0. \quad (4)$$

The initial conditions for the pendulum “displacement” $\eta(t)$ arise from the definition of η and the assumption of zero polarization at the instant of photoexcitation ($t = 0$): zero initial displacement $\eta(0) = 0$, and initial “velocity” set by the Bloch frequency, $\dot{\eta}(0) = \omega_B \equiv e d E_0 / \hbar$. The Bloch frequency does not appear explicitly in Eq. (4), but appears only indirectly through the initial condition.

The pendulum equation describes the transition from plasma oscillations to Bloch oscillations. Integrating Eq. (4) gives the motion of a classical “particle” in a periodic potential $V(\eta) = \omega_p^2 (1 - \cos \eta)$ with a total energy $\omega_B^2 / 2$. For a total energy much smaller than the maximum potential energy ($\omega_B^2 / 2 \ll 2\omega_p^2$), the particle is trapped and oscillates at ω_p in one of the potential minima; the plasmons screen out the external electric field since the Bloch period is larger than half the plasmon period, the time for the screening charges to rearrange. If however the total energy is large ($\omega_B^2 / 2 \gg 2\omega_p^2$), the

particle flies over the washboard potential $V(\eta)$ with velocity $\dot{\eta} = dE(t)$ varying periodically at frequency ω_B ; the plasmons are not fast enough to screen out the external field, so the unscreened field drives the Bloch oscillations. Thus in a THz detection experiment [3] as we vary the external bias, we predict a sudden transition in behavior at $\omega_B = 2\omega_p$ [15] from weakly field dependent to linearly increasing with field (Fig. 1). At the transition point, the motion is aperiodic, leading to a broad frequency spectrum.

The experimental data in Ref. [3] show a Bloch mode that does change to a low field constant frequency mode at 250 GHz; however, this mode has not yet been identified to be plasmonic. In particular, the use of Gaussian beam shapes for photoexcitation leads to lateral carrier inhomogeneities that tend to wash out the plasma frequencies and make them difficult to observe [16].

Coherent LO phonons.—When an ultrafast optical pulse is incident on a polar superlattice, LO phonons are coherently excited [17] by the rapid screening of the static field by photoexcited carriers. On including damping, Eq. (3) modifies to

$$\begin{aligned} \ddot{\eta} + \gamma_{el}(\dot{\eta} - \omega_B) + e^{-\gamma_{el}t} \omega_p^2 \sin \eta &= -C(\dot{w} + \gamma_{el}w), \\ \ddot{w} + \gamma_{ph} \dot{w} + \omega_{TO}^2 w &= C \dot{\eta}, \end{aligned} \quad (5)$$

where γ_{el} and γ_{ph} are the phenomenological damping constants for the electrons and phonons introduced in the microscopic theory. In deriving Eq. (5), we have discarded the electronic memory effects which are unimportant for Bloch-phonon oscillations at low electron density, but must be reintroduced for a proper description of plasmons [18]. Note that the resonance frequency of the phonons is ω_{LO} and *not* ω_{TO} . When the terms linear in w from the right-hand side of the phonon equation are accounted for and the identity $C^2 = \omega_{LO}^2 - \omega_{TO}^2$ is utilized, the resonance frequency can be demonstrated to be ω_{LO} . Prior to photoexcitation, $\dot{\eta}(0) = \omega_B - Cw(0)$ assuming zero initial polarization, and $w(0) = C \dot{\eta}(0) / \omega_{TO}^2$ is the static stretch of the ions in the field. These relations give the following initial conditions: $\eta(0) = \dot{w}(0) = 0$, $\dot{\eta}(0) = \tilde{\omega}_B \equiv \omega_B \epsilon_\infty / \epsilon_0$, and $w(0) = C \tilde{\omega}_B / \omega_{TO}^2 = C \omega_B / \omega_{LO}^2$.

Plasmon phonon.—In the *plasma* limit $\omega_p \gg \omega_B$, we can linearize the sine term in Eq. (5), yielding the familiar plasmon-phonon modes [7]. Reintroducing the memory term that was discarded in Eq. (5) removes the exponential prefactor of the plasma term and leads to a normal damped oscillator response [18]. If the frequencies are plotted versus the electron density at low electronic densities and in the absence of collisions, there is a LO phonon branch and a phonon-renormalized plasmon branch of frequency $\tilde{\omega}_p = \omega_p \sqrt{\epsilon_\infty / \epsilon_0}$. At high densities, the electrons screen the LO phonon mode leading to a bare TO branch and an unrenormalized plasma frequency ω_p . The transition occurs when $\omega_p = \omega_{LO}$ with a gap between the plasmon and phonon modes.

Bloch phonon.—For the nonlinear Bloch limit ($\omega_B \gg \omega_P$), the results are affected by the initial conditions (i.e., the Bloch frequency) derived from the definition of η . In order to make contact with experiments, we model a typical transmission electro-optic spectroscopy measurement. These experiments measure the change in transmission T of a probe pulse [3,8]. The change involves contributions both from the total field $\dot{\eta}(t)$ and the phonon field $w(t)$ through the electro-optic effect [16]:

$$\Delta T/T = r_e \dot{\eta} + r_w w \omega_{LO}^2 / C. \quad (6)$$

The Fourier transform of a numerical solution of Eq. (5) for $\Delta T/T$ with $r_e/r_w = -2.7$ (for bulk GaAs), $\epsilon_0 = 12.9$ and $\epsilon_\infty = 10.9$, reveals a peak at the renormalized Bloch frequency $\tilde{\nu}_B \equiv \tilde{\omega}_B/2\pi = \nu_B \epsilon_\infty / \epsilon_0$ and another at the LO frequency $\nu_{LO} = 8.76$ THz (Fig. 2). Based on the experiments by Dekorsy *et al.* we use the damping times $\gamma_{ph}^{-1} = 1.3$ ps and $\gamma_{el}^{-1} = 0.33$ ps.

Figure 2 shows that there is *no gap* between the Bloch and LO modes when plotted versus the field. This is a consequence of the fact that the Bloch oscillation does not modify the resonant frequencies in Eq. (5), but only controls the initial conditions, i.e., the Bloch oscillations are not elementary excitations of the system. Furthermore there is no response at the TO frequency, which can be understood in the light of the plasmon-phonon discussion. The plasma frequency (electron density) is held constant during the calculation, so the electronic screening is unaf-

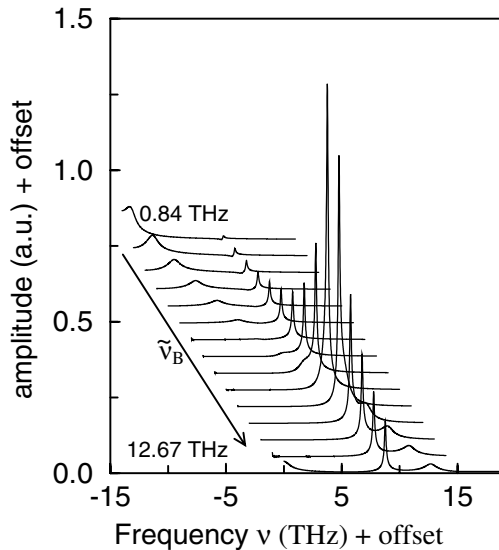


FIG. 2. Bloch-phonon branches in a GaAs/AlGaAs superlattice with $\nu_P = \omega_P/2\pi = 0.5$ THz, for Bloch frequency $\tilde{\nu}_B \equiv \nu_B \epsilon_\infty / \epsilon_0$ varying between 0.84 and 12.67 THz in equal steps. For visual clarity, all graphs are shifted relative to the 12.67 THz data. There is a Bloch branch of frequency $\tilde{\nu}_B$ and a bulk GaAs LO phonon branch, with no discernible gap between them. Moreover, no TO branch arises, in contrast to the plasmon-phonon case. The polar coupling between Bloch oscillations and LO phonons leads to a sharp resonant enhancement of the phonon amplitude.

ected by varying the external field $\sim \omega_B$. There is thus no mechanism for a LO mode to get screened into a mode with a TO frequency.

The coupling between Bloch oscillations and LO phonons is seen in the resonant enhancement of the LO phonon mode in Fig. 2. Figure 3 shows the Fourier amplitudes of the LO phonon and Bloch modes. The LO phonon peak reaches its maximum at the Bloch-phonon resonance $\nu_{LO} = 8.76$ THz for a field-independent damping rate (Fig. 3, set 1).

The absence of a gap and the resonant enhancement of the LO phonon amplitude are in agreement with recent experiments [8] on a superlattice with miniband width (60 meV) larger than the LO phonon energy (36 meV). For these samples, no gap is seen in the Bloch-phonon spectra, while a clear enhancement of the phonon amplitude by the Bloch oscillation is observed. However, the enhancement of the LO peak is shifted by about 1 THz below resonance and in addition a secondary maximum is observed about 1 THz above resonance. This shift and the secondary peak can be explained by introducing a strong field-dependent electronic damping rate γ_{el} near resonance. As argued by Hader *et al.* [19], the electronic damping is maximum near resonance due to increased LO phonon scattering. The electronic damping rate [19] consists of a sharp rise in electron-phonon scattering at resonance followed by an exponential falloff at higher fields. However, for a wide Bloch peak the sharpness of the rise at resonance of the damping rate has to be smoothed over a region corresponding to the width of the Bloch peak below resonance. To demonstrate that

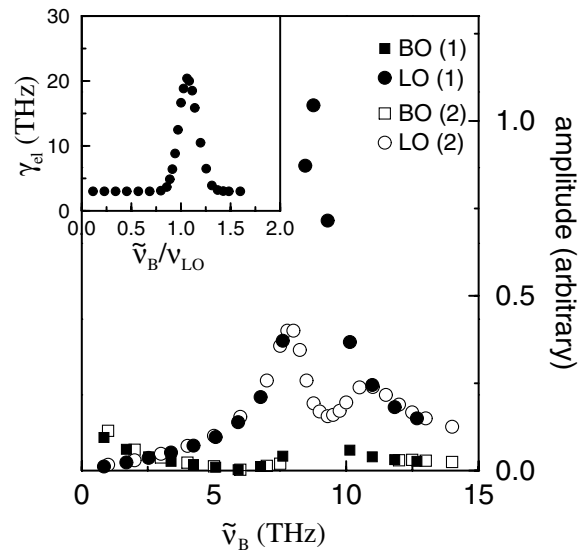


FIG. 3. Amplitudes of Bloch and phonon modes plotted versus the Bloch frequency $\tilde{\nu}_B \equiv \nu_B \epsilon_\infty / \epsilon_0$. Set (1) is for a field-independent electronic damping as in Fig. 2, while set (2) is for the field-dependent γ_{el} as in the inset. Near the phonon resonance at 8.76 THz the Bloch peaks cannot be resolved due to overlap with the phonon peak.

such a damping profile can indeed yield a shifted main phonon peak and a secondary peak, we have made a second calculation including a Hader-like profile at resonance smoothed over the experimental Bloch peak width of about 1.5 THz (inset of Fig. 3). The increased dephasing at resonance decreases the strength of the Bloch oscillator driving the LO mode, leading to the phonon line shape in Fig. 3 (set 2). The calculation shows that the discrepancies between theory and experiment can be explained by a field-dependent electronic damping rate. This conclusion is supported by experiments on a narrow-miniband (36 meV) superlattice where phonon scattering is minimal [8,9]. The electronic collision rate is then roughly field independent, so the shift in the phonon peak below resonance is not strong.

The main features of the Bloch amplitude—a slow initial decrease with increasing field and only a much weaker field dependence near resonance than that for the phonons—are in agreement with the experiments by Dekorsy *et al.* [8]. However, the amplitude of the Bloch peak in Ref. [8] shows a weak maximum below resonance followed by a slow decrease towards resonance, in contrast to our results, which has a minimum at around 6 THz [due to a near cancellation between the total field and the phonon field in Eq. (6)]. Again the details of the Bloch amplitude are sensitive to a possible field-dependent dephasing rate [20]. Further, the experiments reveal TO frequencies that do not exist in our analysis. However, according to Dekorsy *et al.* [8] the TO frequencies arise from plasmon-phonon coupling in the highly doped cladding layers used in the superlattice and vanish for a sample without the doped cladding layers.

In summary, we have numerically solved the coupled equations for Bloch oscillations of electrons in presence of plasmons and phonons. The Bloch oscillations do not produce a gap at resonance with the LO phonons but lead to resonant enhancement of the LO phonon amplitude, as confirmed by experiments. A numerical solution of the coupled Bloch-plasmon-phonon equations predicts a sharp field-dependent transition from coupled plasmon-phonon to Bloch-phonon modes.

This work was supported by the National Science Foundation (PHY-9722127). A. W. G. thanks the Ohio State University Presidential Fellowship for support. We wish to thank A. Bartels, T. Dekorsy, C. Jayaprakash, S. V. Khare, H. Kurz, A. V. Kuznetsov, A. Stahl, and C. J. Stanton for helpful discussions.

*Present address: School of Electrical and Computer Engineering, Purdue University, West Lafayette, IN 47907.

- [1] F. Bloch, Z. Phys. **52**, 555 (1929); C. Zener, Proc. R. Soc. London A **145**, 523 (1934); A. M. Bouchard and M. Luban, Phys. Rev. B **52**, 5105 (1995).
- [2] K. Leo, P. Haring-Bolivar, F. Brüggemann, R. Schwedler, and K. Köhler, Solid State Commun. **84**, 943 (1992).
- [3] T. Dekorsy, P. Leisching, K. Köhler, and H. Kurz, Phys. Rev. B **50**, 8106 (1994).
- [4] M. Ben Dahan, E. Peik, J. Reichel, Y. Castin, and C. Salomon, Phys. Rev. Lett. **76**, 4508 (1996); S. R. Wilkinson, C. F. Bharucha, K. W. Madison, Q. Niu, and M. G. Raizen, Phys. Rev. Lett. **76**, 4512 (1996).
- [5] T. Dekorsy, R. Ott, H. Kurz, and K. Köhler, Phys. Rev. B **51**, 17275 (1995).
- [6] C. Waschke, H. G. Roskos, R. Schwedler, K. Leo, H. Kurz, and K. Köhler, Phys. Rev. Lett. **70**, 3319 (1993).
- [7] A. Mooradian and A. L. McWhorter, Phys. Rev. Lett. **19**, 849 (1967).
- [8] T. Dekorsy *et al.*, preceding Letter, Phys. Rev. Lett. **85**, 1080 (2000).
- [9] T. Dekorsy, A. Bartels, H. Kurz, A. W. Ghosh, L. Jönsson, J. W. Wilkins, K. Köhler, R. Hey, and K. Ploog, Physica (Amsterdam) **7E**, 279 (2000).
- [10] A. W. Ghosh, A. V. Kuznetsov, and J. W. Wilkins, Phys. Rev. Lett. **79**, 3494 (1997).
- [11] The electron-phonon correlations contribute to higher-order processes such as scattering and collision broadening (cf. Ref. [12]).
- [12] T. Kuhn, in *Theory of Transport Properties of Semiconductor Nanostructures*, edited by E. Schöll (Chapman and Hall, London, 1998), p. 181.
- [13] M. Born and K. Huang, *Dynamical Theory of Crystal Lattices* (Clarendon Press, Oxford, 1954).
- [14] É. M. Épshtein, Sov. Phys. Semicond. **11**, 814 (1977).
- [15] Note that for a sample placed between capacitor plates, the Bloch and plasma frequencies in the sample are different from the bare values: $\tilde{\nu}_B \equiv \nu_B \epsilon_\infty / \epsilon_0$ and $\tilde{\nu}_P = \nu_P \sqrt{\epsilon_\infty / \epsilon_0}$.
- [16] A. V. Kuznetsov and C. J. Stanton, Phys. Rev. B **51**, 7555 (1995).
- [17] A. V. Kuznetsov and C. J. Stanton, Phys. Rev. Lett. **73**, 3243 (1994); G. C. Cho, W. Kütt, and H. Kurz, Phys. Rev. Lett. **65**, 764 (1990).
- [18] A. W. Ghosh *et al.* (to be published).
- [19] J. Hader, T. Meier, S. W. Koch, F. Rossi, and N. Linder, Phys. Rev. B **55**, 13799 (1997).
- [20] J. Hader *et al.* [19] predict another step and exponential decay at half the phonon frequency. Our simulations show that this type of profile can produce both a shallow minimum and a weak maximum in the Bloch amplitude.